UDC 54.057:547.995.1

EFFECTS OF ADDITION OF CHITOSAN AND DICARBOXYLIC ACID ON PROPERTIES OF 3D PRINTABLE ACRYLIC RESIN DENTURE BASE

Ihssan F. Al-Takai[1]*, Luma AL-Nema[1], Fawzi H. Jabrail[2]

[1]*Department of Prosthetic Dentistry, College of Dentistry, University of Mosul, Mosul, Iraq.*
[2]*Department of Polymer Chemistry, College of Science, University of Mosul, Mosul, Iraq.*
**Corresponding Author: Ihsan2011@uomosul.edu.iq*

Received 07.11.2023
Accepted 25.01.2024

Abstract: *3D-printing has gained popularity in recent years due to the many advantages it offers over the traditional approaches for instance this technology reduces the time a dentist needs to create and fit dentures to just 2–3 sessions. Fumaric, maleic, and adipic acids with the percentage (0.1 wt.%) were added to chitosan solution (2 wt.%) and the final composite was added to the 3D printable acrylic resin. The specimens were examined for several chemical analyses (XRD, SEM, FTIR) and mechanical tests (impact strength and surface hardness tests), where the total number (115) of specimens used in the study was specimens divided into five groups. In chemical analysis, one specimen was constructed for each modified group and one specimen was used as the control group (3d printable resin without addition (non-modified) for each test. For mechanical tests ten specimens were constructed for each modified group and ten specimens were used as the control group (3d printable resin without addition (non-modified) for each test. The results of chemical analysis showed improvement in the properties of modified 3d printable acrylic denture base resin, additionally the mechanical test results showed that the (Fumaric acid and Maliec acid with Chitosan) specimens have the highest properties in comparison with other specimens, while the lowest properties were for specimens of 3D printable acrylic resin with chitosan. The chemical and mechanical properties of the modified 3D-printed denture base are improved when chitosan is modified with dicarboxylic acids. Conversely, if chitosan alone is used to modify the 3D-printed polymers, the mechanical and chemical properties would be decreased.*

Keywords: *Acrylic resin, Chitosan, Dicarboxylic acids, Fumaric acid, Maleic acid, Adipic acid.*
DOI: 10.32737/2221-8688-2024-1-115-132

1. Introduction

The most popular fabrication techniques that employ the "subtractive" method, in which a solid block of material is cut piece by piece to create the desired object, are casting, molding, forming, and machining. Subtractive methods have evolved significantly over the ages, leading to increased production efficiency and better final product quality [1, 2].

The first chair-side CAD/CAM machines were used in labs and dental offices in the late 1980s. By doing away with the need for impressions, this technology's primary advantage over traditional restorative dentistry techniques was a reduction in chair time. However, the widespread use of dental CAD/CAMs was hindered by the high cost of the equipment and limitations on producing prostheses with precise anatomical details [3,4].

Ciraud created a method for powder deposition of meltable materials in 1972 [2, 5]. *Housholder* developed a laser-assisted powder sintering technique in 1979 using a similar methodology [6]. In contrast to subtractive techniques, these methods use an additive process whereby the objects are constructed layer by layer. 3D Systems Corporation unveiled the first additive manufacturing (AM) equipment in the late 1980s. Since then, AM has

seen a constant rise in applications, primarily in the automotive, aerospace, and medical sectors [7].

Additive manufacturing (AM), known as three-dimensional printing, is a method of creating objects by layer-by-layer material deposition. Aerospace, engineering, construction, and medical are just a few of the industries that use 3D printing. Metals, polymers, and resins are among the many materials that can be used for 3D printing. These substances could be powder, liquid resins, or filaments. 3D printing is being used more and more in biomedical applications, especially in dental and craniofacial applications. Digital dentistry is made possible by the use of 3D printing methods to create patient-specific equipment, such as stereolithography (SLA), fused deposition modeling (FDM), and selective laser sintering. 3D printing for dentistry offers several advantages, including mass and individual customization, precise fit, speedy turnaround times, and accurate clinical results. The most popular type of 3D printable material for dental applications is photo-curable resin. With SLA technology, liquid resin is cured using a scanning laser so that objects can be built layer by layer. LED (light-emitting diode) projectors are used in digital light processing technology to cure the resin. Permanent and temporary crowns, gingiva masks, dental models, surgical guides, and custom impression trays are all made from liquid resin materials processed in SLA or DLP [8].

Photopolymer resin is cured using a projector in the digital light processing (DLP) 3D printing method. The sole distinction between it and Stereolithography (SLA) is that safe-light, or a light bulb, is used to cure the photopolymer resin rather than a UV laser in the SLA 3D printing method [9]. Heat-cured acrylic resin is the material of choice for the construction of complete dentures due to its desirable properties, although it has some disadvantages as its susceptibility to fracture. Several methods and materials are used to reinforce the acrylic resin denture base. One of these methods is reinforcement by using fibers. In this study, visible light cure fiber framework is used as reinforcement material and compared with reinforcement with glass fiber [10].

Compared to heat-polymerized PMMA, the mechanical strength of 3D-printed resin was lower. When CAD/CAM (milled or 3D-printed) materials were compared to conventional denture base material, *Prpic´ et al.* (2020) found that the 3D-printed PMMA had the lowest flexural strength of all the materials tested [11]. This outcome might be the result of the material composition since conventional acrylic resins have a higher double bond conversion rate than the monomer used in 3D printing, which is based on acrylic esters [12].

Surface characteristics were the primary determinant in the selection of denture base materials. Surface properties like surface topography and roughness can affect discoloration, water absorption, microbial adhesion, and even oral hygiene [13]. For clinical applicability, the surface characteristics of 3D-printed DBRs should be evaluated. When compared to traditional heat-polymerized Dentures Base Resins (DBRs), the 3D-printed DBRs had poorer surface characteristics [14].

Many efforts have therefore been undertaken to enhance the mechanical and physical characteristics of printable acrylic resins, and this agrees with Biswas *et al*.,[15] who stated the addition of Filler and nanoparticle-based reinforcing additives to acrylic base resins[16,17]. Chitosan filler is a polycationic polymer that has active “amino” and “hydroxyl” functional groups [18-22]. Moreover, chitosan also has a high resistance to heat due to its intramolecular hydrogen bonds [20, 21], so it can be used safely with printable and thermoplastic resin.

When acrylic resin was mixed with chitosan only, the tensile strength of the resin decreased, but it was still within an acceptable range when compared to the control group that did not add chitosan. These results were consistent with those of other studies that examined the size, aspect ratio, degree of filler dispersion, and adding other filler or materials to the composite [23-25]. This network strengthens the composite material and raises the stress distribution and modulus of elasticity [26] and this might be due to reinforcement and the enhanced interfacial bonding effect of chitosan composites which dispersed in resin

due to their high surface area, producing a network-like structure and restrict polymer chain mobility in the resin matrix, increasing the stiffness and modulus of elasticity [26-28].

The acrylic resin without mixture (control) had the largest average number of pores compared with the acrylic resin mixed with chitosan and acrylic acid at 1 and 2% concentrations. This phenomenon occurred because even after the polymerization of acrylic resin without a mixture, some monomers did not bind to the polymer and instead formed pores. Meanwhile, acrylic acid can function as a coupling agent to form bonds between acrylic resin and chitosan; hence, the monomers contained in the acrylic resin can be bonded during polymerization [29].

This finding was confirmed by the decreased residual monomer quantity in the acrylic resin mixtures with 1 and 2% chitosan and acrylic acid [30]. Therefore, this polymerization can reduce the formation of pores. The decrease in the amount of residual monomer can reduce the formation of space known as porosity [29]. A large pore size will allow the easy absorption of liquid, which in turn will reduce the density and other mechanical properties of the acrylic resin [31, 32].

This study aimed to evaluate the effects of adding chitosan, both pure chitosan solution and the composite of chitosan with a dicarboxylic acid, on the various characteristics of a 3D printable acrylic resin denture base.

2. Materials and methods

2.1. Materials.

The materials with their origin state and short description are tabulated below (**Table 1**).

Table 1. Materials used in the study

Chitosan powder (Shrimp source, China),DD=75-85%; M.Wt=190-310KDa;glacial acetic acid was supplied by Darmstadt, Germany
Fumaric acid (glacial 100%, pro-analysis) was purchased from Merck (Darmstadt, Germany).
Adipic acid (glacial 100%, pro analysis) was obtained from Sigma-Aldrich (USA).
Maleic acid (glacial 100%, pro-analysis) was purchased from Sigma Al-drich (USA)
Poly(vinyl alcohol) (PVA Fluka), Honeywell Fluka, M.Wt=195 Kg mol^{-1}
Ultrapure water (Maxima UltraPure Water, Elga-Prima Corp, UK) with resistivity > 18 MΩ/cm
3d printable acrylic resin (DENTABASE 3D+ denture base material (ASIGA , Australia)

2.2. Preparation

2.2.1. Chitosan Solution preparation. A commercial supplier provided the chitosan solution. With a deacetylation percentage (DD) of 75–85% from chitin that will be processed, a local company sold shrimp source chitosan powder (China). Every solution was prepared using ultra-pure water. Every experiment used freshly made solutions, and no additional purification was applied to any of the chemicals. An oven was used to dry the chitosan until a consistent weight was reached. Dry chitosan (0.1 g) was dissolved in (2 wt%) of acetic acid solution in Ultra-pure water.

The solution was stirred and heated to 60 degrees Celsius for (I hour) and after completely dissolved, the solution was filtered for removal of air bubbles and undissolved materials [33].

2.2.2. Chitosan with dicarboxylic acid solutions. Dry chitosan solution (1.0g) was dissolved in the following acid solutions (2wt%) adipic acid, maleic acid, fumaric acid, then gently stirred, and heated to approximately 55°C in an oven for an entire night for dissolving and then filtered to get rid of any remaining dust and other contaminants and left two hours at room temperature for removal air bubbles from the solutions [33].

Subsequently, 0.1ml of each modified Chitosan acid solution was added to the main weight of the 3D printable acrylic resin (Asiga washing and curing machine; Australia). The designs are saved as STL files, and after the base and support are added to the 3D-designed samples, the printer settings and slicing are adjusted before the samples are exported to the

printer. Additionally, the study's recommendations for slice thickness, specimen cleaning, and drying were all followed [34, 35].

The specimens were ready for chemical and physical testing following the modification procedures. Thus, approximately 115 specimens were used in the study. ANOVA, Duncan's multiple range tests, mean and standard deviation, and $p \leq 0.01$ were used to identify significant differences between the tested groups.

2.3. Chemical analysis

2.3.1. Field Emission Scanning Electron Microscopy (SEM). The surface structure and distribution of the nanoparticles were assessed using a scanning electron microscope (SEM) with a spatial resolution of 1.5 nm (Mira 3 Tescan FESEM, Czech). Using a sputter coating machine, a 20 μm layer of gold was applied to all 3D printed samples to make them electroconductive and suitable for SEM imaging scanning. (15 KeV) is the accelerating voltage, and the magnification power will range from 2000 to 5000 X [36].

2.3.2. Fourier Transform Infrared Spectroscopy (FTIR). Fourier Transform Infrared Spectroscopy of a CL Alpha-PFTIR spectrophotometer with a wavenumber range of 400–4000 cm^{-1} and a resolution of 2 cm^{-1} will be used to perform FTIR.

2.3.3. X- Ray Diffraction (XRD). An XRD instrument with CuKα tube operating at 40 kV and 30 mA produces X-rays with a wavelength of λ=1.54060Å; the scan mode is continuous scan, and the scanning speed is 5deg/min.

2.4. Mechanical test

2.4.1. Impact Strength

An impact strength test was performed using a Charpy impact tester. The test specimens were prepared following the ISO standard No. 179, measuring 55×10×10±0.2mm for length, width, and height, respectively, and featuring a V-shaped notch. The specimen's notch measured 2.5 mm in depth, with an effective depth of 7.5 mm below the notch throughout its 10 mm width. The specimen was fixed horizontally using two support arms spaced 40 mm apart. It was then struck by a 75.8 kg free-swinging pendulum that was released from a fixed height at the midpoint on the opposite side of the notch. The impact strength of each specimen was measured in kJ/m^2 using the formula below [37, 38]:

$$\text{Impact strength} = E/b*d$$

(here, *E*: absorbed energy, *b*: sample width, *d*: sample thickness).

2.4.2. Surface Hardness:

The following dimensions (10×10×3.3±0.2 mm for length, width, and height, respectively) will be prepared for each group's specimens. Every specimen had five measurements made on various parts of it, from which the mean value was determined [39].

The Microhardness Vickers tester (HV-1000A, Korea) will be used to measure the specimen's surface hardness. The hard materials are fitted with an indenter, which is a 1.25 mm-diameter round steel ball [40].

The apparatus's solid plane will hold the specimen, and the needle is positioned 12 mm from the specimen's edge. A constant minor load of 44.5N was applied to the specimens. The apparatus automatically converted the tester's measurement of the indenter's relative movement, which is measured immediately after each indentation, into a scale with a graduation of 0 to 100 units. After the load is applied for one second, the final hardness value will be determined by visually interpreting the analog.

3. Results and discussions

3.1 Field Emission Scanning Electron Microscopy (SEM).

In this test, the SEM images showed that chitosan samples only form an irregular morphological surfaces with folds and voids with high porosity and the chitosan surfaces show high roughness which means high shape factors with whiten spots or edges mean they had course surfaces, while with the addition of 2% w/w chitosan to dicarboxylic acids (adipic,

fumaric, and maleic acids) SEM images shows a homogenous structure after addition of chitosan and dicarboxylic acid materials more than that of the control samples and the chitosan samples alone (**Figure 1**).

The morphology of the examined samples studied by SEM shows major morphologic features and a microstructure overview were observed at low magnification, precise morphological features was observed at medium magnification, and microstructural details were observed at high magnification [41].

The 3D printable acrylic resin was analyzed using FESEM. The modified resin with chitosan alone and chitosan with dicarboxylic acids caused observable morphological changes.

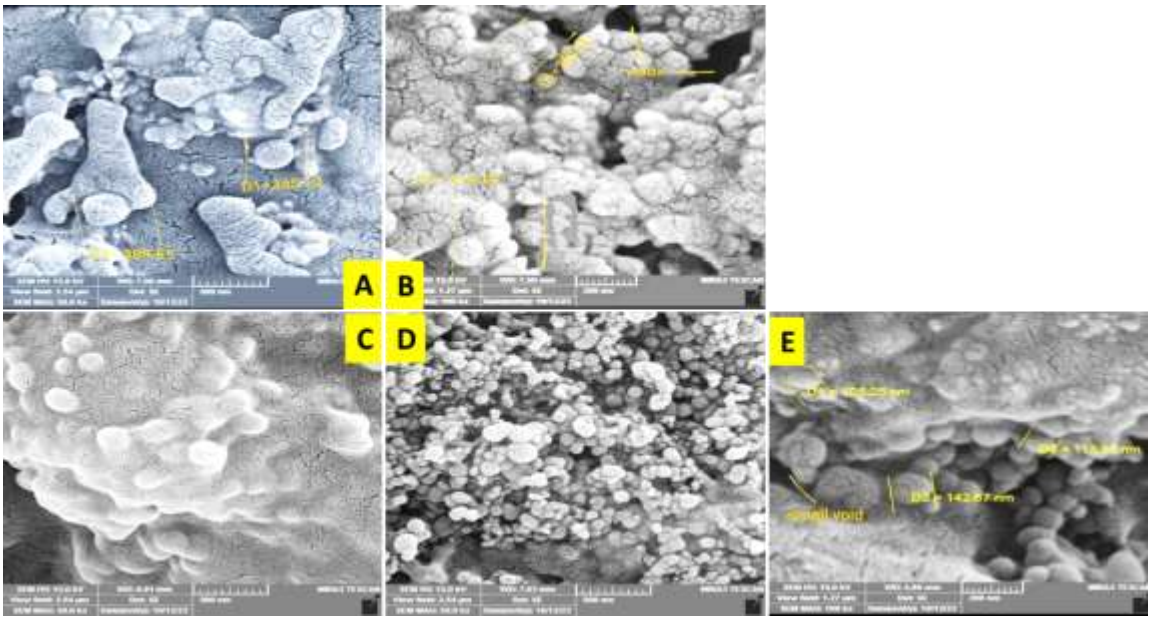

Fig. 1. A representatiove images of Field Emission Scanning Electron Microscopy of (A) Control group; (B) Chitosan group; (C) Adipic acid group; (D) Fumaric acid group; (E) Maleic acid group.

The large-sized particles of the modified samples had irregular surface morphology, while the surface of the unmodified control sample was rough. The surface morphology of the control samples showed pores, which suggested that the material had not been compacted with fatigue composite.

The control sample's surface morphology showed 42 pores, which increased when chitosan was added, showing chitosan particles with less dispersion of 3d printable acrylic resin.

The SEM image of 2% w/w chitosan alone showed that the chitosan particles had embedded themselves in the denture base resin. This could have an impact on the physical or mechanical bond that can form because of size differences between the chitosan and the resin; this could be because the resin is unable to bind with all of the chitosan particles, and the voids in the polymerized resin can cause the strength to decrease as the chitosan percentage increases [42].

SEM pictures were used to support the conclusions. Furthermore, the dispersion of particles in space and the development of multilayer coupling agents surrounding the particles may limit the availability of functional groups for monomer reactions.

When analyzing various concentrations of different denture base composites, the earlier studies [24; 43-46] observed a decrease in flexural strength due to non-uniform distribution and insufficient binding of composite particles in the resin matrix. The extended hydrocarbon chain of adipic acid may be the reason for the increased adhesion and homogeneity of 3D printable resin particles observed in the FESEM images of the chitosan: adipic acid group.

FESEM images of the chitosan: fumaric acid samples revealed that the particles had a

more spherical, crystalline structure, which indicates that the cohesiveness of the 3D-printed resin particles increased and the overall material structure became more compact.

The maleic acid group displayed the most compact and homogenous morphological surface in the FESEM images, and the modified polymer demonstrated extremely high strength and compactness figures owing to its configuration. In line with [41] who claimed that a compact microstructure generated by PMMA particles diffusing toward one another to form strong connection necks because of the photopolymerization process in the PMMA sample, the dicarboxylic acid samples used in this study had a compact microstructure generated by 3D printable PMMA resin particles diffusing toward one another, leading to the holes and voids decreasing, increasing overall resistance and compactness, and forming strong connection necks following a successful and flawless photopolymerization process.

This is in line with Qin et al. [47], who stated that the interaction of chitosan with other biomaterials, like nanodiamonds, is important to improve its biological and mechanical properties for clinical applications where these interactions showed higher color stability compared with other materials. Additionally, the interaction of chitosan with other biomaterials, like dicarboxylic acids, is important to improve its biological and mechanical properties for clinical applications.

3.2. Fourier Transform Infrared Spectroscopy (FTIR).

The FTIR spectrum of control samples which represent the acrylic resin, shows absorption bands at 2955cm^{-1} and 2872cm^{-1} are related to aliphatic υ(C–H) groups. The strong absorption bands at 1715cm^{-1} and 1082cm^{-1} represent the υ(C=O) group and the υ(C-O) group, respectively. The strong absorption bands at 3369cm^{-1} were belong to the hydroxyl group υ(O-H) group, in addition, the absorption bands at 1405 cm^{-1} and 1387cm^{-1} are related to δ(-CH_2) groups of acrylic resin (**Figure 2**).

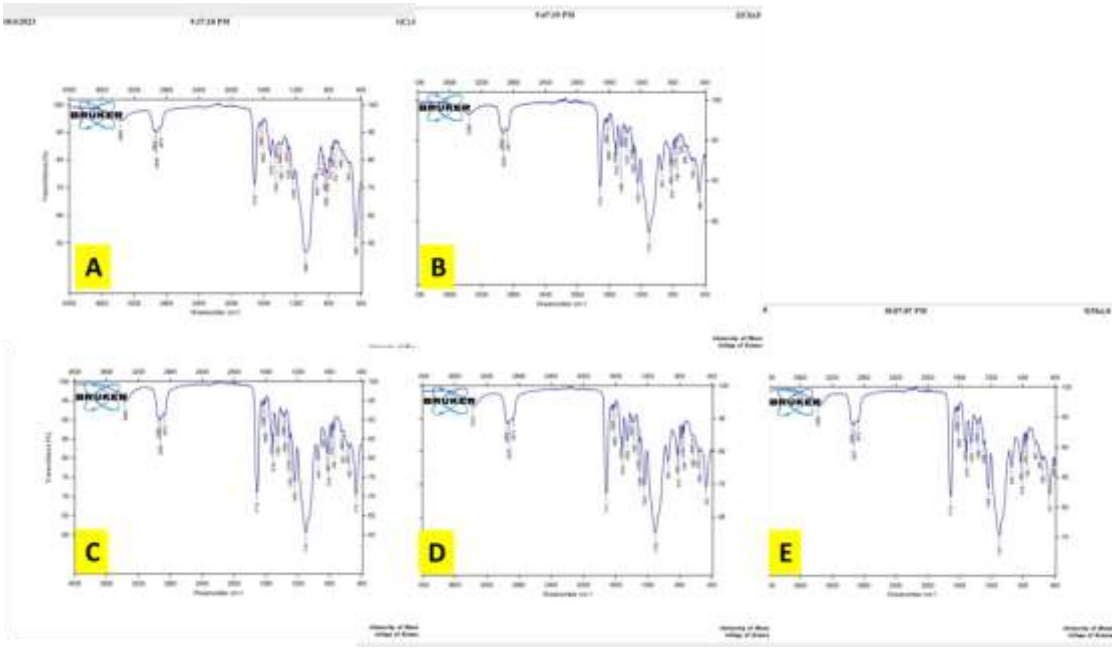

Fig. 2. A representative images of Fourier Transform Infrared Spectroscopy (A) Control group; (B) acrylic resin modified only with 2%(w/w) Chitosan alone; (C) acrylic resin modified with chitosan and adipic acid; (D) acrylic resin modified with chitosan and fumaric acid; (E) acrylic resin modified with chitosan and maleic acid

The FTIR spectrum of acrylic resin modified only with 2%(w/w) Chitosan alone shows absorption bands at 2955 cm^{-1} and 2871cm^{-1} are related to the aliphatic υ(C–H) group. The strong absorption bands at 1715 cm^{-1} and 1510 cm^{-1} represent the υ(C=O) group and

υ(N-H) group of amide-I and amide-II of chitosan. The absorption frequency at 1101cm^{-1} belongs to υ(C-O) and that at 3360 cm^{-1} represent the hydroxyl group υ(O-H) group in acrylic resin and chitosan. Those bands at 1405 cm^{-1} and 1377 cm^{-1} are related to δ(-CH_2) groups of acrylic resin.

The FTIR spectrum of acrylic resin modified with chitosan and adipic acid shows absorption bands at 2955 cm^{-1} and 2872 cm^{-1} are related to the aliphatic group υ(C–H). The absorption bands at 1713 cm^{-1} and 1510 cm^{-1} are representing the υ(C=O) group and υ(N-H) group of amide-I and amide-II of chitosan respectively. The absorption bands at 1101cm^{-1} and 3368 cm^{-1} for υ(C-O) and υ(O-H) groups, respectively. The absorption bands at 1384 cm^{-1} and 1366 cm^{-1} are related to δ(-CH_2) groups of acrylic resin.

The FTIR spectrum of acrylic resin modified with chitosan and fumaric acid shows absorption bands at 2955 cm^{-1} and 2872 cm^{-1} are related to the aliphatic group υ(C–H). The absorption bands at 1714 cm^{-1} and 1510 cm^{-1} represent the υ(C=O) and υ(N-H) groups of amide-I and amide-II of chitosan respectively. The absorption bands at 1103 cm^{-1} and 3374 cm^{-1} belong to υ (C-O) and υ(O-H) groups respectively. In addition, the absorption bands at 1404 cm^{-1} and 1367 cm^{-1} are related to the δ(-CH_2) group of acrylic resin.

The FTIR spectrum of acrylic resin modified with chitosan and maleic acid shows absorption bands at 2954 cm^{-1} and 2872 cm^{-1} are related to the aliphatic group υ(C–H). The absorption bands at 1713 cm^{-1} and 1510 cm^{-1} represent the υ(C=O) and υ(N-H) groups of amide-I and amide-II of chitosan, respectively. The absorption bands at 1101 cm^{-1} and 3380 cm^{-1} belong to υ (C-O) and υ(O-H) groups, respectively. In addition, the absorption bands at 1384 cm^{-1} and 1366 cm^{-1} are related to the δ(-CH_2) group of acrylic resin.

FTIR analysis was employed to determine whether epoxy groups are present in acrylic latex and to investigate the interaction of chitosan and acrylic latex during the mixing process [48]. When engineered chitosan polysaccharide interacts with dicarboxylic acids, functional group modifications are monitored through FTIR studies. Comparing the dicarboxylic acid spectrum to the chitosan group alone revealed few discernible changes. The result of superposed -OH was a broad, strong absorption in the 3380-3368 cm^{-1} region. The aliphatic group ϋ(C–H) is connected to the absorption bands at 2954 cm^{-1} and 2872 cm^{-1}.

The presence of asymmetric -COO− stretching is indicated by absorptions in the 1713–1715 cm^{-1} range. The peak that was seen between 1510 and 1500 cm^{-1} was caused by stretching of the symmetric N-H bend. Further absorption peaks at 1387, 1082, and 1405 cm^{-1} were similar to the chitosan 2% spectrum, suggesting that the main structural backbone of the chitosan structure did not change [49].

FTIR analyses confirm the interaction of dicarboxylic acids with chitosan and the results suggested that the concentration of dicarboxylic acids, increases the degree of cross-linking with chitosan and this agrees with Sailakshmi *et al.* [50] who stated that FTIR spectral analyses confirm the interaction of dicarboxylic acids with chitosan polysaccharide and the results suggested that increase in the concentration of DCA (0.05%-0.5%), increases the degree of cross-linking up to 0.4% concentration and about 60%-65% cross-linking was observed with 0.2% DCA with chitosan

3.3. X- Ray Diffraction (XRD)

The XRD pattern showed that the maxima of the control group occurred at (16.561 degrees) along the 2Θ axis with a width of maxima (0.161) and a height of maxima (468) which improved that the samples of the control group had an amorphous shape, while the maxima of the chitosan samples added alone present at (18.62 degrees) along the 2Θ axis with more height of maxima (449)and width of maxima was (0.086) which less than that of the control samples, and this means that the chitosan group had more crystalline behavior than the control group and all other group used in the study (**Table 2, Figure 3**).

The XRD pattern also showed that the maxima of adipic acid samples occurred at (17.439 degrees) along the 2Θ axis with a width of maxima (0.262) and height of maxima (275) which improve that the samples of adipic acid had an amorphous shape more than that of the control group and only chitosan group 2% w/w. The XRD pattern also showed that the

maxima of fumaric acid samples occurred at (17.730 degrees) along the 2Θ axis with a width of maxima (0.315) and height of maxima (454) which improved that the samples of fumaric acid had highly amorphous texture more than that of all other group used in the study. The XRD pattern also showed that the maxima of maleic acid samples occurred at (16.830 degrees) along the 2Θ axis with a width of maxima (0.297) and height of maxima (354) which improved that the samples of maleic acid had highly amorphous texture more than that of all other group used in the study except fumaric acid group.

Table 2. Peak Search Report (1 Peaks, Max P/N=4.0) for tested groups.

Groups	2-Theta	d (spacing)	BG	Height	I%	Area	I%	FWHM (width)
Control	16.561	5.3485	1395	468	100	9436	100	0.161
Chitosan	18.620	4.7614	1351	449	100	4854	100	0.086
Adipic acid	17.439	5.0812	929	275	100	9247	100	0.262
Fumaric acid	17.730	4.9983	1466	454	100	17883	100	0.315
Maleic acid	16.830	5.2636	1520	354	100	13131	100	0.297
PEAK: 47-pts/Parabolic Filter, Threshold=3.0, Cutoff=2.0%, BG=3/1.0, Peak-Top=Summit								

The degree of crystallinity, element proportions in the mixture, and crystallinity of the specimens are all determined by XRD analysis. Part of the ray may be transmitted through atomic planes when an X-ray interacts with a material; the remaining portion is absorbed, refracted, scattered, and diffracted by the specimens. Depending on the atomic arrangement and type, materials' X-ray diffraction patterns vary for each element [51].

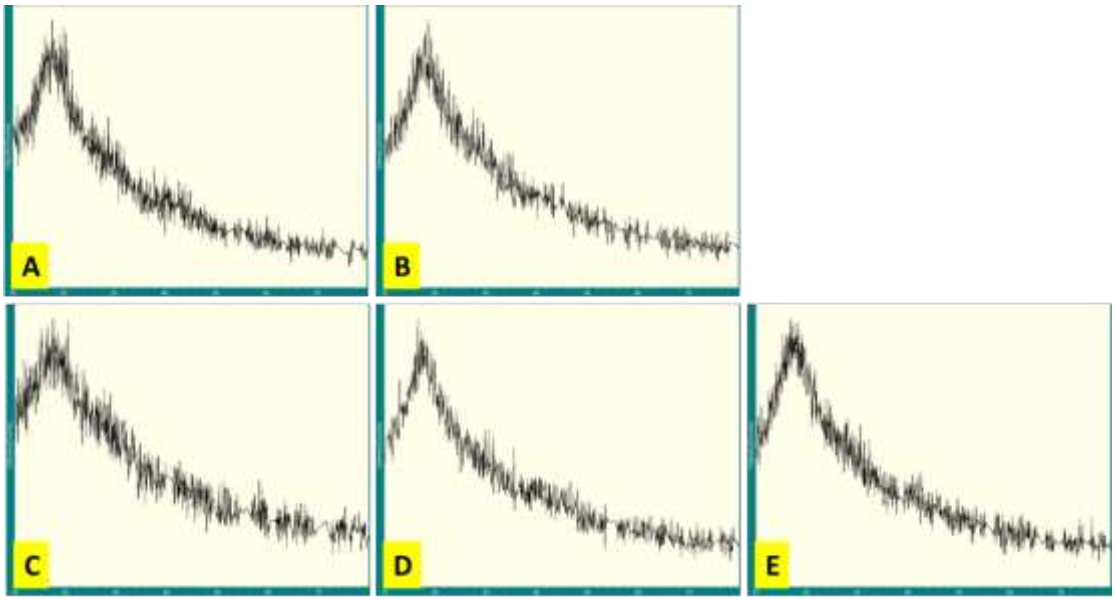

Fig. 3. Representative images of X-Ray Diffraction of (A) Control group; (B) Chitosan group; (C) Adipic acid group; (D) Fumaric acid group; (E) Maleic acid group.

Since XRD displays the normal order of crystalline phases of the materials under investigation, it was utilized to analyze the impact of the incorporated polymers on the PMMA crystallinity behavior [52, 53]. The XRD pattern of control samples showed a single diffraction peak, signifying the material's amorphous nature. The control group samples had an amorphous shape that corresponded to the amorphous region of the material, as evidenced by the broad diffraction peak at 16.561 degrees along the 2θ axis, with width of maxima (0.161) and height of maxima (468) [54]. The XRD pattern of chitosan samples

alone had more intensity and sharpness with narrower diffraction peaks than those of the control group in the amorphous region, indicating that the addition of chitosan to polymer improved the crystallinity and structural configuration of PMMA, which had a direct impact on its mechanical, biological, and physical properties. However, chitosan samples alone at (18.62 degrees) along the 2θ axis with more height of maxima (449) and width of maxima (0.086) was less than that of the control group. These results agree with Salman *et al*. [40] reported that the XRD graph displayed narrower peaks and increased intensity as the polymer's crystallinity increased.

The XRD pattern of dicarboxylic acid with chitosan showed a broader diffraction peaks with less intensity and sharpness than that appeared in the XRD pattern of control group, indicating that the addition of dicarboxylic acid with chitosan to 3D printable acrylic resin confirms that there was no apparent chemical interaction between the blended material and there was only physical (electrostatic) interaction between the added agent which could form amorphous architectural build with 3D printable acrylic resin due to the formation of interpenetrating network among the blended composite [55-57]. So, that the XRD pattern improved that control group and the group of dicadboxylic acid with chitosan 2% w/w were highly amorphous and with no any crystalline maxima.

3.2 Mechanical test results and discussion.

3.2.1. Impact strength. The impact test mean and standard deviation values for the control, experimental, and modified groups. According to the results, the control sample's impact was greater than that of the experimental group modified with only 2 wt % chitosan and less than that of the experimental sample modified with the dicarboxylic acid used in the study (adipic, fumaric, and maleic acid and chitosan). The modification by the maleic acid group resulted in the highest impact value (18.7). This study revealed a highly significant statistical difference between the impact of the modified groups and the control group, with P-value≤0.01(**Table 3**).

Using Duncan's multiple range values showed that the impact value of the 3D printable acrylic denture base modified with Chitosan (12.4) was lower than that of the control group (15.9), whereas the impact value of the base modified with dicarboxylic acid (Adipic, Fumaric, and Malic acid) + Chitosan (16, 18.7, and 18.7) was higher. The 3D printable acrylics modified with Chitosan samples showed a statistically significant difference from the control group (**Table 4**). Additionally, there was a statistically significant difference between the control sample and the sample of fumaric acid and maleic acid on one side, as well as a statistically significant difference between the samples of fumaric acid and maleic acid on one side and the Chitosan sample on the other side. However, there was no statistically significant difference between the control group and the samples of 3D printable acrylics modified with adipic acid, nor between the samples of fumaric acid and maleic acid on the other.

Table 3. Impact of control and experimental groups which modified with a dicarboxylic acid (Adipic, Fumaric, and Maleic acid and Chitosan) and with only Chitosan 2 wt%.

Test in 15/9	Subgroup	Mean±SD
Impact Test	Control, n=10	15.9±0.7b
	Chitosan, n=10	12.4±0.7a
	Adipic, n=10	16±0.6b
	Fumaric, n=10	18.7±0.7c
	Maleic, n=10	18.7±0.8c
Same letter=non-significant difference (p>0.05) Different letter=significant difference (p<0.05)		

Table 4. Impact of control and experimental groups which modified with a dicarboxylic acid (Adipic, Fumaric, and Maleic acid and Chitosan) and with only Chitosan 2 wt%.

	Sum of Squares	Df	Mean Square	F	Sig.
Between Groups	268.021	4	67.005	140.767	0.000**
Within Groups	21.420	45	.476		
Total	289.441	49			
** Highly Significant at P-Value ≤ 0.01, ANOVA test					

In terms of the modified materials' mechanical properties, these are essential characteristics of any biomaterial from an application standpoint [50]. The foundation materials for dentures should be sufficiently impact-resistant to withstand fracture in the event of an unintentional drop. Maxillary denture fractures are mostly caused by impact and fatigue forces, whereas impact forces account for 80% of mandibular denture fractures. Using the Charpy or Izod configurations, impact strength tests are frequently used to assess the amount of energy absorbed by materials before fracture [45, 58, 59].

The maximum augmentation in the impact strength was achieved after the addition of maleic fumaric and adipic acids respectively (18.7, 18.66, and 16 KJ/m^2). The difference in impact strength decreased between the fumaric acid samples and maleic acid samples which was in the range of impact strength values which were approximately the same, so that there was no statistically significant difference.

The impact strength obtained from a mixture of a dicarboxylic acid with a concentration of 0.1% with resin matrix containing chitosan 2 wt %was found to be higher than that of the standard 3D printable acrylic resin without modification (control) and the only chitosan samples. This can be attributed to the fact that the mixture of two added materials can produce a mixture of materials containing the properties of the two components such that other properties tend to make the mixture material into a matrix with better strength properties.

This can be seen in the 3d acrylic resin matrix mixture with chitosan and dicarboxylic acid which shows an increase in impact strength and this agrees with *Sailakshmi et al*. [50] who approved that the most preferable mechanical properties were observed at 0.2% concentration of dicarboxylic acid and any additional increase in DCA concentration results in the reduction in mechanical properties. The crossed carbon double bonds react with the oligomer during the reaction as it polymerized, forming bonds with the filler into a polymer matrix. This bond can add strength to the nature of physical strength, namely impact strength [31].

The noteworthy association between impact strength variables and residual monomer variables provides an additional explanation. The impact strength variable and the residual monomer variable had a correlation coefficient of -0.6682. The opposite relationship between the two variables is indicated by a negative correlation coefficient. The impact strength decreases with increasing residual monomer concentration and vice versa. According to *Feng et al.* [60], the acrylic resin may become more plastic and lose impact strength due to the leftover monomer acting as a plasticizer, so that the results of this study suggest that the addition of carboxylic acid to acrylic resin lead to decrease the residual monomer elution and this point lead to increase the impact strength of the modified dicarboxylic samples.

A statistically significant increase in the impact strength of the modified groups compared to the control group was confirmed by One Way Analysis of Variance at $p \leq 0.01$. The findings showed that the presence of acidic content enhanced the mechanical properties (impact strength) of the resulting polymer and that chitosan and dicarboxylic acids increased the chain's length and strength. The carboxyl derivatives of diacid interacted with the NH_2 group of chitosan through covalent or physical linkage, improving the mechanical properties over those of the control samples, even though all of these observations showed the cross-linking ability of dicarboxylic acid with chitosan [50, 61].

This agrees with *Prajwala et al*. [62] who approved that the impact strength of the resin matrix improved when it was incorporated by rubbery particles as the crack propagation was decelerated when reached the rubber interface. This also was in agreement with *Gad and Abualsaud* [63] who reported that the properties of composites are greatly influenced by the interactions between the polymer matrix and the incorporated fillers.

Ayaz and Durkan [64] asserted that the high strength of compatibility between the components of the crosslinked polymeric blend was disrupted by the excess polymer incorporated or that the increase in porosity was the cause. This is supported by the observation of a decrease in the impact strength of 3D PMMA along with the addition of chitosan alone. This result could be attributed to supersaturation of the polymer matrix and the excess of added chitosan filler. Denture fractures were found to be primarily caused by porosity and stress concentration [65]. This is consistent with the findings of *Anjali et al*. [66], who discovered that the impact strength of the composite is mainly determined by the filler particle distribution within the matrix. Furthermore, the outcomes supported the findings of *Spasojevic et al.* [67], who linked the decreased impact strength of modified resin materials to the emergence of microdefects in the polymer matrix, which act as a stress concentrator and crack accelerator.

3.2.2. Surface Hardness. According to the findings, the control group's surface hardness was higher than that of the experimental samples modified with chitosan 2 wt % alone and lowers than that of the experimental samples modified with the dicarboxylic acid used in the study (adipic, fumaric, and malic acid) and chitosan. With the addition of the fumaric acid samples, the maximum surface hardness value of 48.20 was attained. The surface roughness of the modified samples differed statistically significantly from the control samples at p value≤0.01 (**Table 5**).

According to Duncan's multiple range values, the modified 3D printable acrylic denture base with chitosan 2 wt % alone had a lower surface hardness (20.659) compared to the control samples (30.650); on the other hand, the modified 3D printable acrylic denture base with dicarboxylic acid (Adipic, Fumaric, and Malic acid) and Chitosan had a higher surface hardness (32.440, 41.220, and 39.100), respectively and all modified samples—aside from the samples that was modified with adipic acid showed a statistically significant difference in surface hardness from the control samples. The study also showed a statistically significant difference in surface hardness among all modified samples, with the exception of the groups that were modified with fumaric and maleic acids, which showed no statistically significant difference in surface hardness between them (**Table 6**).

Table 5. Surface hardness of tested groups.

Test	Subgroup	Mean±SD
Hardness Results	Control, n=10	30.7±5.9b
	Chitosan, n=10	20.7±6.7a
	Adipic, n=10	32.5±3.1b
	Fumaric, n=10	41.2±7.3c
	Maliec, n=10	39.1±4.7c
Same letter=non-significant difference (p>0.05) Different letter=significant difference (p<0.05)		

Table 6. Surface hardness of control and experimental groups which modified with dicarboxylic acid (Adipic, Fumaric and Maleic acid and Chitosan) and with Chitosan 2wt % alone.

	Sum of Squares	Df	Mean Square	F	Sig.
Between Groups	2627.414	4	656.854	**19.889**	**0.000****
Within Groups	1486.201	45	33.027		
Total	4113.615	49			

** Highly Significant at P-Value ≤ 0.01, ANOVA test

The results of surface hardness can be explained by stating that according to the result of FESEM images which shows an increased adhesion and homogeneity of the chitosan-adipic acid samples, and revealed that in the chitosan-furmaric acid samples the particles had a more spherical, crystalline structure, which indicates that the cohesiveness of the 3D-printed resin particles increased and the overall material structure became more compact. The maleic acid group displayed the most compact and homogenous morphological surface in the FESEM images, and the modified polymer demonstrated extremely high strength and compactness owing to its configuration. The dicarboxylic acid samples used in this study had a compact microstructure generated by 3D printable PMMA resin particles diffusing toward one another, which led to the holes and voids decreasing, increasing overall resistance and compactness, and forming strong connection necks following a successful and flawless photopolymerization process. This is consistent with another study [41] who claimed that a compact microstructure generated by PMMA particles diffusing toward one another to form strong connection necks because of the photopolymerization process in the PMMA sample, while certain voids were discovered at the fracture site of the 3D-printed specimens with chitosan 2% alone, according to SEM results. These gaps could weaken the bonding layers between surfaces, which could cause delamination and fractures. As a result, it was determined that voids had a role in the printed resin's decreased mechanical performance. Furthermore, the kind of failure observed depends on where the voids are located. If a void is in the center of the specimen, it will function as a flaw; if it is on the edges of the specimen, it may function as the fracture's starting point and reduce hardness [68, 69].

Another explanation was that the complex mixture was intended to be reinforced by the addition of dicarboxylic acid (DCA). Chitosan and acrylic resin may bind actively to the hydroxyl group of acrylic acid. Double bonds (C = O) and two carboxylic acids (COOH) were present in dicarboxylic acid (DCA). If there is any residual monomer left over from the reaction of an acrylic resin mixture between a polymer and a monomer, it will be reduced by adding chitosan and dicarboxylic acid. Acidic carboxylates react with NH2 from base chitosan, while the acrylic acid double bond (C=O) reacts with acrylic resin monomers, the residual monomer showed a decrease in the percentage of residual monomer. This was due to the acrylic resin's monomers binding to form polymer bonds during polymerization. The residual monomer decreased as the degree of bond conversion increased under UV light and by the addition of additive to acrylic resin and this finding agrees with *Al-Ali et a*l. [70] who stated that the degree of bond conversion increased when curing was done under high temperatures as in microwave or heat curing method and the light cure resin showed the highest degree of bond conversion and agree with *Hasan and Abdulla* [71] whom stated that the application of fiber to polymer during mixing to form a polymer monomer matrix, the monomer seems to be reduced, so the level of tested residual monomer seems to be the low level in groups of heat and miocrowaved reinforced resin with fibers than the non-reinforced resins. Residual monomers can also lessen the mechanical strength and surface hardness of acrylic resins and these finding agree with *Anusavice et al.* [72] and *Chaves et al*. [73].

4. Conclusions

The chemical and mechanical properties of the modified 3D-printed denture base are improved when 2 wt.% chitosan is modified with fumaric acid + 2wt.% chitosan and maleic acid+2 wt.% chitosan groups have the highest mechanical properties than other groups in the study. When chitosan 2 wt.% alone was used to modify the 3D-printed polymers, the mechanical and chemical properties would be decreased.

The FTIR spectrum shows that the chitosan cross-linked dicarboxylic acids blend the acrylic resin. Moreover, SEM images show homogeneous structures after blending with observable morphological changes, while a 3D printable acrylic resin after blending with chitosan alone shows an irregular surface morphology.

The degree of crystallinity was improved after blending especially in the case of fumaric and maleic acid cross-linked chitosan additive.

The impact strength and surface hardness were increased significantly and improved for 3D printable acrylic resin after modification especially in case of fumaric and maleic acid cross-linked chitosan additive.

Acknowledgements
The authors acknowledge the College of Dentistry, Mosul University in Iraq for providing support in performing this research.

Conflicts of interest: There is no Conflict of interest

Ethical approval and consent to participate: REC reference no. UOM. Dent. 23/38

References

1. Kalpakjian S., Schmid S.R., Musa H. Manufacturing engineering and technology: hot Processe. *China Machine Press.* 2011. 1180 p.
2. Tayebi L., Masaeli R., Zandsalimi K., Tayebi L., Masaeli R., Zandsalimi K. 3D printing methods applicable in oral and maxillofacial surgery. *In Book:* 3D Printing in Oral & Maxillofacial Surgery. 2021. pp.11-60.
3. Miyazaki T., Hotta Y., Kunii J., Kuriyama S., Tamaki Y. A review of dental CAD/CAM: current status and future perspectives from 20 years of experience. *Dental materials journal.* 2009. vol. 28(1). pp. 44-56.
4. Poticny D.J., Klim J. CAD/CAM in-office technology: innovations after 25 years for predictable, esthetic outcomes. *The journal of the American dental association.* 2010. vol. 141, pp.5-9.
5. Ciraud P.A. Process and Device for the Manufacture of any Objects Desired from any Meltable Material. FRG Disclosure Publication. 1972, 2263777.
6. Housholder R.F. Molding process. Google Patents. 1981/
7. Zhai Y., Lados D.A., LaGoy J.L. Additive manufacturing: making imagination the major limitation. *Jom.* 2014, 66, p. 808-16.
8. Belsure N., Parekh S., Soni N. An Overview of 3D Printable Materials for Dental and Craniofacial Applications. 3D Printing in Oral Health Science: // Applications and Future Directions. 2022, 27, p. 69-91.
9. Stansbury J.W., Idacavage M.J. 3D printing with polymers: Challenges among expanding options and opportunities. *Dental materials.* 2016, vol. 32, no. 1. P. 54-64.
10. AL-Omari A.W. Visible Light Cure Fiber Frame Work Reinforcement of Acrylic Resin Denture Base Material. A Comparative Study. *Al-Rafidain Dental Journal.* 2014, vol. 14, no. 2, pp. 173-81.
11. Prpić V., Schauperl Z., Ćatić A., Dulčić N., Čimić S. Comparison of mechanical properties of 3D-printed, CAD/CAM, and conventional denture base materials. *Journal of Prosthodontics*. 2020, vol. 29, no. 6, p. 524-8.
12. Alifui-Segbaya F., Bowman J., White A.R., George R., Fidan I. Characterization of the double bond conversion of acrylic resins for 3D printing of dental prostheses. *Compendium.* 2019, vol. 40, no.10, p. e7-e11
13. Shim J.S., Kim J.E., Jeong S.H., Choi Y.J., Ryu J.J. Printing accuracy, mechanical properties, surface characteristics, and microbial adhesion of 3D-printed resins with various printing orientations. *The*

Journal of prosthetic dentistry. 2020, vol. 124, no. 4, p. 468-75 .
14. Al-Dulaijan Y.A., Alsulaimi L., Alotaibi R., Alboainain A., Alalawi H., Alshehri S., Khan S.Q., Alsaloum M., AlRumaih H.S., Alhumaidan A.A., Gad M.M. Comparative Evaluation of Surface Roughness and Hardness of 3D Printed Resins. *Materials.* 2022, vol. 15, no. 19, p. 6822 .
15. Biswas S.K., Shams M.I., Das A.K., Islam M.N., Nazhad M.M. Flexible and transparent chitin/acrylic nanocomposite films with high mechanical strength. *Fibers and Polymers.* 2015, no.16, p. 774-81.
16. Ergun G., Sahin Z., Ataol A.S. The effects of adding various ratios of zirconium oxide nanoparticles to poly(methyl methacrylate) on physical and mechanical properties. *Journal of oral science*. 2018, vol.60, no.2, p. 304-15.
17. Sha B.Y., Liu Q.S., Cheng L., Yin X.Y. Preparation and Application of Core-shell PMMA/Chitosan Nanoparticle. *Advanced Materials Research.* 2012, V. 535, p. 271-4 .
18. Topouzi M., Kontonasaki E., Bikiaris D., Papadopoulou L., Paraskevopoulos K.M., Koidis P. Reinforcement of a PMMA resin for interim fixed prostheses with silica nanoparticles. *Journal of the mechanical behavior of biomedical materials*. 2017, vol. 69, pp. 213-22 .
19. Gad M., ArRejaie A.S., Abdel-Halim M.S., Rahoma A. The reinforcement effect of nano-zirconia on the transverse strength of repaired acrylic denture base. *International journal of dentistry.* 2016, vol. 2016, Article ID 7094056
20. Nam K.-Y., Shin Y.-M. Antifungal effect and characterization of denture PMMA impregnated with chitosan. *Korean Journal of Dental Materials.* 2017, vol. 44, no.2, pp. 87-94.
21. Onishi H., Machida Y. Biodegradation and distribution of water-soluble chitosan in mice. *Biomaterials.* 1999, vol. 20, no.2, p.175-82 .
22. Wieckiewicz M., Boening K.W., Grychowska N., Paradowska-Stolarz A. Clinical application of chitosan in dental specialities. Mini reviews in medicinal chemistry. 2017, vol. 17, no.5, p. 401-9 .
23. Kikuchi L.N., Freitas S.R., Amorim A.F., Delechiave G., Catalani L.H., Braga R.R., Moreira M.S., Boaro L.C., Gonçalves F. Effects of the crosslinking of chitosan/DCPA particles in the antimicrobial and mechanical properties of dental restorative composites. *Dental Materials.* 2022, vol. 38, no.9, pp. 1482-91 .
24. Al-Harbi F.A., Abdel-Halim M.S., Gad M.M., Fouda S.M., Baba N.Z., AlRumaih H.S., Akhtar S. Effect of nanodiamond addition on flexural strength, impact strength, and surface roughness of PMMA denture base. *Journal of Prosthodontics*. 2019, vol. 28, no.1, pp. 417-25.
25. Milovanović A., Sedmak A., Golubović Z., Mihajlović K.Z., Žurkić A., Trajković I., Milošević M. The effect of time on mechanical properties of biocompatible photopolymer resins used for fabrication of clear dental aligners. *Journal of the mechanical behavior of biomedical materials.* 2021, vol.119, 104494 .
26. Husseinsyah S., Amri F., Husin K., Ismail H. Mechanical and thermal properties of chitosan-filled polypropylene composites: The effect of acrylic acid. // Journal of Vinyl and Additive Technology. 2011, vol. 17, no.2, p. 125-31.
27. Woźniak A., Biernat M. Methods for crosslinking and stabilization of chitosan structures for potential medical applications. *Journal of Bioactive and Compatible Polymers.* 2022, vol. 37, no.3, pp. 151-67 .
28. Paradowska-Stolarz A., Wezgowiec J., Malysa A., Wieckiewicz M. Effects of Polishing and Artificial Aging on Mechanical Properties of Dental LT Clear® Resin. *Journal of Functional Biomaterials*. 2023, vol. 14, no. 6, p. 295.
29. Ismiyati T., Alhasyimi A.A. Effect of Chitosan and Acrylic Acid Addition to Acrylic Resin on Porosity and Streptococcus mutans Growth in Denture Base. *European Journal of Dentistry*. 2023, vol.17, no.3, pp. 693-698.
30. Wicaksono S., Rezkita F., Wijaya F.N., Nugraha A.P., Winias S. Ellagic acid: an alternative for antifungal drugs resistance in

HIV/AIDS patients with oropharyngeal candidiasis. HIV & AIDS Review. *International Journal of HIV-Related Problems*. 2020, vol.19, no.3. pp. 153-6 .
31. Ismiyati T., Alhasyimi A.A. The effect of chitosan addition in acrylic resin matrix towards the residual monomers and impact strength. Research Journal of Pharmacy and Technology. 2021, vol.14, no. 4, pp. 2280-5.
32. Pero A.C., Marra J., Paleari A.G., Pereira W.R., Barbosa D.B., Compagnoni M.A. Measurement of interfacial porosity at the acrylic resin/denture tooth interface. *Journal of Prosthodontics: Implant, Esthetic and Reconstructive Dentistry*. 2010, vol.19, no.1, pp. 42-6.
33. El-Hefian E.A., Nasef M.M., Yahaya A.H. The preparation and characterization of chitosan/poly (vinyl alcohol) blended films. E-*journal of chemistry*. 2010, vol. 7, no.4, pp. 1212-9.
34. Herpel C., Tasaka A., Higuchi S., Finke D., Kühle R., Odaka K., Rues S., Lux C.J., Yamashita S., Rammelsberg P., Schwindling F.S. Accuracy of 3D printing compared with milling—A multi-center analysis of try-in dentures. *Journal of Dentistry*. 2021, vol. 110, p. 103681.
35. Zeidan A.A., Sherif A.F., Baraka Y., Abualsaud R., Abdelrahim R.A., Gad M.M., Helal M.A. Evaluation of the Effect of Different Construction Techniques of CAD-CAM Milled, 3D-Printed, and Polyamide Denture Base Resins on Flexural Strength: An In Vitro Comparative Study. *Journal of Prosthodontics.* 2023, vol. 32, no. 1, pp. 77-82.
36. Muralidhar G., Satish Babu C.L., Shetty S. Integrity of the interface between denture base and soft liner: A scanning electron microscopic study. *The Journal of Indian Prosthodontic Society*. 2012, vol. 12, pp. 72-7.
37. Asar N.V., Albayrak H., Korkmaz T., Turkyilmaz I. Influence of various metal oxides on mechanical and physical properties of heat-cured polymethyl methacrylate denture base resins. *The journal of advanced prosthodontics*. 2013, vol. 5, no.3, pp. 241-7.
38. Gad M.M., Fouda S.M., ArRejaie A.S., Al-Thobity A.M. Comparative effect of different polymerization techniques on the flexural and surface properties of acrylic denture bases. *Journal of Prosthodontics.* 2019, vol. 28, no.4. pp. 458-65.
39. Song S.Y., Kim K.S., Lee J.Y., Shin S.W. Physical properties and color stability of injection-molded thermoplastic denture base resins. *The journal of advanced prosthodontics.* 2019, vol. 11, no.1, pp. 32-40.
40. Salman A.D., Jani G.H., Fatalla A.A. Comparative study of the effect of incorporating SiO_2 nano-particles on properties of poly methyl methacrylate denture bases. *Biomedical and Pharmacology Journal.* 2017, vol. 10, no. 3, pp. 1525-35.
41. Barbur I., Opris H., Crisan B., Cuc S., Colosi H.A., Baciut M., Opris D., Prodan D., Moldovan M., Crisan L., Dinu C. Statistical comparison of the mechanical properties of 3D-printed resin through triple-jetting technology and conventional PMMA in orthodontic occlusal splint manufacturing. // Biomedicines. 2023, V. 11, no.8, p. 2155 .
42. Chander N.G., Venkatraman J. Mechanical properties and surface roughness of chitosan reinforced heat polymerized denture base resin. *Journal of Prosthodontic Research.* 2022, vol. 66, no.1, pp. 101-8.
43. Karci M., Demir N., Yazman S. Evaluation of flexural strength of different denture base materials reinforced with different nanoparticles. *Journal of Prosthodontics*. 2019, vol. 28, no. 5, pp. 572-9 .
44. Maitra U., Prasad K.E., Ramamurty U., Rao C.N. Mechanical properties of nanodiamond-reinforced polymer-matrix composites. // Solid State Communications. 2009, V. 149, no. 39-40, p. 1693-7 .
45. Abdulwahhab S.S. High-impact strength acrylic denture base material processed by autoclave. *Journal of prosthodontic research.* 2013, vol. 57, no. 4, pp. 288-93.
46. Sodagar A., Bahador A., Khalil S., Shahroudi A.S., Kassaee M.Z. The effect of

TiO_2 and SiO_2 nanoparticles on flexural strength of poly (methyl methacrylate) acrylic resins. Journal of prosthodontic research. 2013, V.57, no. 1, p. 15-9.
47. Qin C., Xiao Q., Li H., Fang M., Liu Y., Chen X., Li Q. Calorimetric studies of the action of chitosan-N-2-hydroxypropyl trimethyl ammonium chloride on the growth of microorganisms. *International journal of biological macromolecules*. 2004, vol. 34, no. 1-2, pp. 121-6.
48. Torabi S., Mahdavian A.R., Sanei M., Abdollahi A. Chitosan and functionalized acrylic nanoparticles as the precursor of new generation of bio-based antibacterial films. *Materials Science and Engineering*: C. 2016, vol. 59, pp. 1-9.
49. Pavia D.L., Lampman G.M., Kriz G.S., Vyvyan J.A. Introduction to spectroscopy. Cengage learning; 2014, Department of Chemistry Western Washington University Bellingham, Washington . 786 p.
50. Sailakshmi G., Mitra T., Chatterjee S., Gnanamani A. Engineering chitosan using α, ω-dicarboxylic acids—an approach to improve the mechanical strength and thermal stability. *Journal of Biomaterials and Nanobiotechnology*. 2013, vol.4, no.2, pp. 151-164
51. Korin E., Froumin N., Cohen S. Surface analysis of nanocomplexes by X-ray photoelectron spectroscopy (XPS). *ACS Biomaterials Science & Engineering.* 2017, vol.3, no.6, pp. 882-9.
52. Ataol A.S., Ergun G., Abdulrazzaq Naji S., Behroozibakhsh M., Jafarzadeh Kashi T.S., Eslami H., Masaeli R., Mahgoli H., Tahriri M., Ghavvami Lahiji M., Rakhshan V. Effects of incorporation of 2.5 and 5 wt% TiO_2 nanotubes on fracture toughness, flexural strength, and microhardness of denture base poly methyl methacrylate (PMMA). *The journal of advanced prosthodontics.* 2018, vol.10, no.2, pp. 113-21 .
53. Gopalakrishnan S., Thomas S., Kalazikkal N. OSC21: Morphological, Mechanical and Biological Properties of Silver Nanoparticle Decorated Denture Base Polymer. *The Journal of Indian Prosthodontic Society.* 2018, vol.18(Suppl 1), p. S16.
54. Vasubabu M., Jeevan Kumar R., Ramprasad T., Rekha E. Thermal Analysis on Acrylic Based Denture Materials. *Biomed. J., Sci. Tech. Res*. 2017, vol.1, no.7, pp. 1-3.
55. Tomar A.K., Mahendia S., Kumar S. Structural characterization of PMMA blended with chemically synthesized PAni. *Adv. Appl. Sci. Res*. 2011, vol.2, no.3, pp. 327-33.
56. Motaung T.E., Luyt A.S., Bondioli F., Messori M., Saladino M.L., Spinella A., Nasillo G., Caponetti E. PMMA–titania nanocomposites: properties and thermal degradation behaviour. *Polymer Degradation and Stability.* 2012, vol. 97, no. 8, pp. 1325-33.
57. Jalil A., Khan S., Naeem F., Haider M.S., Sarwar S., Riaz A., Ranjha N.M. The structural, morphological and thermal properties of grafted pH-sensitive interpenetrating highly porous polymeric composites of sodium alginate/acrylic acid copolymers for controlled delivery of diclofenac potassium. *Designed Monomers and Polymers.* 2017, vol.20, no. 1, pp. 308-24.
58. Gad M.M., Alshehri S.Z., Alhamid S.A., Albarrak A., Khan S.Q., Alshahrani F.A., Alqarawi F.K. Water sorption, solubility, and translucency of 3D-printed denture base resins. *Dentistry Journal.* 2022, vol.10, no.3, p. 42.
59. Kraemer Fernandez P., Unkovskiy A., Benkendorff V., Klink A., Spintzyk S. Surface characteristics of milled and 3D printed denture base materials following polishing and coating: An in-vitro study. *Materials.* 2020, vol.13, no. 15, p. 3305.
60. Feng D., Gong H., Zhang J., Guo X., Yan M., Zhu S. Effects of antibacterial coating on monomer exudation and the mechanical properties of denture base resins. *The Journal of prosthetic dentistry.* 2017, vol. 117, no.1, pp. 171-7.
61. Huf S., Krügener S., Hirth T., Rupp S., Zibek S. Biotechnological synthesis of long-chain dicarboxylic acids as building blocks for polymers. *European Journal of Lipid Science and Technology*. 2011, vol.113, no.5, pp. 548-61.

62. Prajwala N., Kumar C.R., Sujesh M., Rao D.C., Pavani L. Denture base reinforcing materials-A review. *IP Ann. Prosthodont. Restor. Dent.* 2020, no. 6, pp. 52-9.
63. Gad M.M., Abualsaud R. Behavior of PMMA denture base materials containing titanium dioxide nanoparticles: A literature review. *International journal of biomaterials*. 2019, vol.17, p. 2019.
64. Aydogan Ayaz E., Durkan R. Influence of acrylamide monomer addition to the acrylic denture-base resins on mechanical and physical properties. *International Journal of Oral Science.* 2013, vol.5, no. 4, pp. 229-35.
65. Bora P., Vikhe D., Bhandari A., Namita Gandhi N. Reinforced Single Complete Maxillary Denture. *Oral Health Dentistry*. 2018, vol.3, no.3, pp. 648-652 .
66. Malik R., Bhandari S., Pant A., Saxena A., Kumar N., Chotrani N., Gunwant D., Sah P.L. Fabrication and mechanical testing of egg shell particles reinforced Al-Si composites. *International Journal of Mathematical, Engineering and Management Sciences*. 2017, vol. 2, no.1, p. 53.
67. Spasojevic P., Zrilic M., Panic V., Stamenkovic D., Seslija S., Velickovic S. The mechanical properties of a poly (methyl methacrylate) denture base material modified with dimethyl itaconate and di-n-butyl itaconate. *International Journal of Polymer Science*. 2015, vol. 2015, Article ID 561012.
68. Wang X., Jiang M., Zhou Z., Gou J., Hui D. 3D printing of polymer matrix composites: A review and prospective. *Composites Part B: Engineering*. 2017, vol.110, pp. 442-58.
69. Väyrynen V.O., Tanner J., Vallittu P.K. The anisotropicity of the flexural properties of an occlusal device material processed by stereolithography. *The Journal of Prosthetic Dentistry.* 2016, vol.116, no.5, pp. 811-7.
70. Al–Ali A.A., Sheet O.A., Taqa A.A. The effect of different curing techniques on the degree of bond conversion for different types of acrylic resin materials. *Al-Rafidain Dental Journal*. 2013, vol.13, no.2, p. 351-357
71. Hasan R.H., Abdulla M.A. Reinforced Microwave-Cured Acrylic Resin Denture Base Material with Glass Fibers. // Al-Rafidain Dental Journal. 2010, V.10, no.2, pp. 314-21.
72. Anusavice K.J., Shen C., Rawls H.R., editors. Phillips' science of dental materials. Elsevier Health Sciences; 2012, Sep 27.
73. Chaves C.D., Machado A.L., Vergani C.E., de Souza R.F., Giampaolo E.T. Cytotoxicity of denture base and hard chairside reline materials: a systematic review. *The Journal of prosthetic dentistry.* 2012, vol.107, no.2, pp. 114-27.

XİTOZAN VƏ DİKARBON TURŞULARININ ƏLAVƏLƏRİNİN DİŞ PROTEZLƏRİNİN 3D ÇAPINDA İSTİFADƏ OLUNAN AKRİL QATRANININ XASSƏLƏRİNƏ TƏSİRİ

İhsan F. Əl-Təkai[1]*, Luma Əl-Nema[1], Fauzi H. Cəbrayıl[2]

[1] Mosul Universiteti, Stomatologiya Kolleci, Protez Diş Müalicəsi Departamenti, Mosul, İraq.
[2]Mosul Universiteti, Elmlər Kolleci, Polimer Kimyası Departamenti, Mosul, İraq.
**e-mail: Ihsan2011@uomosul.edu.iq*

Xülasə: 3D çap texnologiyası ənənəvi yanaşmalarla müqayisədə bir çox üstünlüklərə görə son illərdə populyarlıq qazanmışdır. Məsələn, bu texnologiya diş həkiminin diş protezlərinin hazırlanması üçün lazım olan vaxtı 2-3 seansa qədər azaldır. Fumar, malein və adipin turşuları (0.1 kütlə %) xitozan məhluluna (2 kütlə %), son kompozit isə 3D çap üçün uyğun olan akril qatranına əlavə edilir. Nümunələr bir neçə kimyəvi analiz (XRD, SEM, FTIR) və mexaniki sınaqlarla (zərbəyə davamlılıq və səthi möhkəmlik testləri) xarakterizə edilmişdir. Bu tədqiqatda istifadə edilən nümunələrin ümumi sayı (115) beş qrupa bölünmüşdür. Kimyəvi analiz üçün bir nümunə

hazırlanmış və bir nümunə nəzarət qrupu kimi istifadə edilmişdir (hər test üçün əlavəsiz 3D çap qatranı (dəyişdirilməmiş)). Mexaniki sınaq üçün hər bir dəyişdirilmiş qrup üçün on nümunə hazırlanmış və on nümunə nəzarət qrupu kimi istifadə edilmişdir (hər sınaq üçün əlavələrsiz 3D çap qatranı (dəyişiklik edilməmiş). Kimyəvi analizlərin nəticələrində dəyişdirilmiş akril 3D çap qatranının təkmilləşdirilmiş xüsusiyyətləri müşahidə olunmuşdur. Bundan əlavə, mexaniki sınaqların nəticələri göstərmişdir ki, nümunələri digər nümunələrlə müqayisədə fumar turşusu və xitoanlı malein turşusu ən yüksək xassələrə, ən aşağı xüsusiyyətlər isə 3D çap üçün nəzərdə tutulmuş xitozanlı akril qatrandan hazırlanmış nümunələrə aiddir. Çap protezləri xitozan istifadə edilməklə təkmilləşdirilmiş və dikarbon turşularla modifikasiya edilmişdir. Əksinə, 3D çap edilmiş polimerləri dəyişdirmək üçün yalnız xitozan istifadə edilərsə, mexaniki və kimyəvi xassələri azalacaq.

Açar sözləri: akril qatranı, xitosan, dikarbon turşuları, fumarin turşusu, malein turşusu, adipin turşusu.

ВЛИЯНИЕ ДОБАВКИ ХИТОЗАНА И ДИКАРБОНОВЫХ КИСЛОТ НА СВОЙСТВА АКРИЛОВОЙ СМОЛЫ ДЛЯ 3D ПЕЧАТИ ОСНОВАНИЯ ЗУБНЫХ ПРОТЕЗОВ

Ихсан Ф. Аль-Такай[1]*, Лума Аль-Нема[1], Фаузи Х. Джабраил[2]

[1]Кафедра ортопедической стоматологии, Стоматологический колледж, Университет Мосула, Мосул, Ирак.
[2]Кафедра химии полимеров, Научный колледж Мосульского университета, Мосул, Ирак.
**e-mail: Ihsan2011@uomosul.edu.iq*

Аннотация: 3D-печать приобрела популярность в последние годы благодаря множеству преимуществ, которые она предлагает по сравнению с традиционными подходами. Например, эта технология сокращает время, необходимое стоматологу для создания и установки зубных протезов, до 2–3 сеансов. Фумаровую, малеиновую и адипиновую кислоты в процентном соотношении (0.1 мас.%) добавляли к раствору хитозана (2 мас.%), а конечный композит добавляли к акриловой смоле, пригодной для 3D-печати. Образцы были подвергнуты нескольким химическим анализам (XRD, SEM, FTIR) и механическим испытаниям (испытания на ударную вязкость и поверхностную твердость), где общее количество (115) образцов, использованных в исследовании, представляло собой образцы, разделенные на пять групп. При химическом анализе был изготовлен один образец для каждой модифицированной группы, и один образец использовался в качестве контрольной группы (смола для 3D-печати без добавок (немодифицированная) для каждого испытания). Для механических испытаний было изготовлено десять образцов для каждой модифицированной группы и десять образцов были использованы в качестве контрольной группы (смола для 3D-печати без добавок (немодифицированная) для каждого теста. Результаты химического анализа показали улучшение свойств модифицированной акриловой смолы для 3D-печати, кроме того, результаты механических испытаний показали, что (фумаровая кислоты и малеиновой кислоты с хитозаном) образцы имеют самые высокие свойства по сравнению с другими образцами, а самые низкие свойства были у образцов из акриловой смолы с хитозаном, предназначенной для 3D-печати. Химические и механические свойства модифицированного 3D-печатного протеза улучшаются при использовании хитозана. Модифицируется дикарбоновыми кислотами. И наоборот, если для модификации полимеров, напечатанных на 3D-принтере, использовать только хитозан, механические и химические свойства будут снижены.

Ключевые слова: акриловая смола, хитозан, дикарбоновые кислоты, фумаровая кислота, малеиновая кислота, адипиновая кислота.